

Aberystwyth University

The Cryogenian record in the southern Kingston Range, California

Le Heron, Daniel P.; Busfield, Marie; Ali, Dilshad Omer; Tofaif, Saeed; Vandyk, Thomas Matthew

Published in:
Precambrian Research

DOI:
[10.1016/j.precamres.2017.07.017](https://doi.org/10.1016/j.precamres.2017.07.017)

Publication date:
2018

Citation for published version (APA):
Le Heron, D. P., Busfield, M., Ali, D. O., Tofaif, S., & Vandyk, T. M. (2018). The Cryogenian record in the southern Kingston Range, California: the thickest Death Valley succession in the hunt for a GSSP. *Precambrian Research*, 319, 158-172. <https://doi.org/10.1016/j.precamres.2017.07.017>

General rights

Copyright and moral rights for the publications made accessible in the Aberystwyth Research Portal (the Institutional Repository) are retained by the authors and/or other copyright owners and it is a condition of accessing publications that users recognise and abide by the legal requirements associated with these rights.

- Users may download and print one copy of any publication from the Aberystwyth Research Portal for the purpose of private study or research.
- You may not further distribute the material or use it for any profit-making activity or commercial gain
- You may freely distribute the URL identifying the publication in the Aberystwyth Research Portal

Take down policy

If you believe that this document breaches copyright please contact us providing details, and we will remove access to the work immediately and investigate your claim.

tel: +44 1970 62 2400
email: is@aber.ac.uk

Accepted Manuscript

The Cryogenian record in the southern Kingston Range, California: the thickest Death Valley succession in the hunt for a GSSP

Daniel Paul Le Heron, Marie Elen Busfield, Dilshad Omer Ali, Saeed Tofaif, Thomas Matthew Vandyk

PII: S0301-9268(17)30078-5
DOI: <http://dx.doi.org/10.1016/j.precamres.2017.07.017>
Reference: PRECAM 4827

To appear in: *Precambrian Research*

Received Date: 14 February 2017
Revised Date: 3 July 2017
Accepted Date: 18 July 2017

Please cite this article as: D.P.L. Heron, M.E. Busfield, D.O. Ali, S. Tofaif, T.M. Vandyk, The Cryogenian record in the southern Kingston Range, California: the thickest Death Valley succession in the hunt for a GSSP, *Precambrian Research* (2017), doi: <http://dx.doi.org/10.1016/j.precamres.2017.07.017>

This is a PDF file of an unedited manuscript that has been accepted for publication. As a service to our customers we are providing this early version of the manuscript. The manuscript will undergo copyediting, typesetting, and review of the resulting proof before it is published in its final form. Please note that during the production process errors may be discovered which could affect the content, and all legal disclaimers that apply to the journal pertain.



1 **The Cryogenian record in the southern Kingston Range,**
2 **California: the thickest Death Valley succession in the hunt for a**
3 **GSSP**

4
5 Daniel Paul Le Heron^{1†}, Marie Elen Busfield², Dilshad Omer Ali¹, Saeed Tofaif¹, Thomas
6 Matthew Vandyk¹.

7 ¹*Department of Earth Sciences, Royal Holloway University of London, Egham, Surrey, TW20*
8 *OEX*

9 ²*Department of Geography and Earth Sciences, Llandinam Building, Aberystwyth University,*
10 *SY23 3DB*

11
12 **ABSTRACT**

13 The Kingston Peak Formation of the Death Valley area, California, allows valuable insight
14 into both regional Cordilleran stratigraphy and the number of glacial cycles preserved in the
15 Cryogenian record. In the Kingston Range, the eponymous strata have been previously
16 interpreted to record both Sturtian and Marinoan pan-glacial events. In the context of a search
17 for a Global Boundary Stratotype Section and Point (GSSP) for the Cryogenian, we provide
18 the first detailed description of the thickest diamictite-bearing interval in the western USA.
19 Two clast-poor, muddy diamictite intervals within the succession- one at the base, and one
20 near the top- have been used to support Sturtian and Marinoan events previously. However,
21 new data from the southern part of the Kingston Range suggest that the upper diamictite
22 interval is genetically related to underlying strata. The deposits are interpreted as glaciogenic
23 debris flow deposits which probably represent the proximal tract of a subaqueous fan. Medial
24 to distal portions of this fan are dominated by turbidites, which were transported down a
25 consistent SE-oriented palaeoslope. Lowermost beds of the upper diamictite interval are
26 intercalated with graded sandstones and sandy, matrix supported conglomerates. The graded
27 beds (turbidites) and matrix-supported conglomerates (debrites) testify to a subaqueous
28 setting, with the compositionally and texturally distinct diamictites indicating a glacial origin.

29
30
31
32
33
[†]daniel.le-heron@rhul.ac.uk

34 1. Introduction

35 A major priority for Precambrian research is the establishment of a suitable and
36 representative Global Boundary Stratotype Section and Point (GSSP) for the Cryogenian
37 period (Shields-Zhou et al., 2016). Current thinking suggests that GSSPs should be chosen by
38 physic-chemical markers, rather than having any biostratigraphic basis (Smith et al., 2015). In
39 this context, we present a case study of the thickest hitherto published example of a
40 Cryogenian diamictite succession in the Death Valley region, California, USA (**Fig. 1**). We
41 consider the evolution of this succession in terms of the number of glacial cycles preserved
42 by comparison to successions in neighbouring outcrop belts, and in terms of the
43 “completeness” of its record. The succession of diamictite-bearing rocks of the Kingston
44 Peak Formation described in this paper are 2.5 km thick, and represent the thickest known
45 accumulations of Cryogenian glacially-related strata in the western USA. Prior to a recent
46 study in the Silurian Hills, (approximately 30 km to the SW of the study area) where 1.4 km
47 of diamictite-bearing strata were measured (Le Heron et al., 2017), it was thought that the
48 thickest accumulation of Cryogenian diamictites cropped out in the Panamint Range
49 immediately west of Death Valley (Miller, 1985; Prave et al., 1999). Indeed, prior to the
50 present contribution, the thickest known accumulations in the western USA were reported
51 from the Dutch Peak Formation in the Sheeprock Mountains of Utah (Christie-Blick et al.,
52 1982). In general terms, owing to the likely duration of time over which these rocks
53 accumulated (possibly 55 Ma: Rooney et al., 2015), it is probable that they record much
54 lower accumulation rates (perhaps 4-15 times slower) than either Palaeozoic or Cenozoic
55 glacial successions (Partin and Sadler, 2016).

56 The Kingston Peak Formation is of global significance as it is an exceptional archive
57 for Cryogenian climate cycles. Ever since Hazzard (1933) recognised evidence for glacial
58 deposition in the Kingston Peak Formation of the Death Valley area (then regarded as
59 Cambrian in age), various attempts have been made to establish the significance of these
60 deposits in a wider regional and ultimately global context. Miller (1985) argued for two
61 phases of glaciation in strata of the Panamint Range immediately west of Death Valley, with
62 basalts within the middle of the succession (Labotka et al., 1980) cited as archetypal evidence
63 for two phases of Rodinian rift margin development (Prave, 1999). Prave (1999) provided an
64 overview of the formation throughout the Death Valley area, using outcrops in the Panamint
65 Range in particular to argue for a two-phased glaciation allied to two phases of continental
66 rifting. The popular two-phased model was revived in Macdonald et al. (2013), who also

67 argued that discrete phases of glaciation had produced discrete tectonostratigraphic units
68 which could then be correlated across the US Cordillera as isochronous time markers. The
69 earlier phase of glaciation was proposed to be Sturtian in age, whereas the later phase of
70 glaciation was allied to the Marinoan glaciation of South Australia (Macdonald et al., 2013).
71 Based on a very detailed investigation of the Silurian Hills, Le Heron et al. (2017) identified
72 four main packages of glacial diamictite interbedded with slope-derived olistostrome
73 material, hence casting doubt on the universal applicability of a two-fold glaciation, and
74 raising questions about which study area, if any, should be regarded as a representative
75 archive of the Cryogenian glacial record.

76

77 **2. Previous work and context**

78 Prave (1999) proposed a regional stratigraphy for the Kingston Peak Formation (KPF), which
79 saw it divided into three ascending stratigraphic units (KP1-3). The lowermost of these (KP1)
80 comprises monotonous siltstone and sandstone intercalations that are devoid of any evidence
81 for a glacial influence and hence considered genetically unrelated to the overlying strata. KP2
82 comprises a laterally extensive diamictite unit (Prave, 1999). The overlying unit (KP3) was
83 argued to represent a glacial retreat. Macdonald et al. (2013) adopted similar interpretations
84 to Prave (1999), developing the idea that units KP2-KP3 represented the record of the
85 Sturtian pan-glacial. These authors slightly misquoted both Wright (1954) and Prave (1999)
86 to whom they attributed a new stratigraphic unit (KP4) at the top of the succession. However,
87 whilst the origins of a fourfold stratigraphic subdivision can be traced to Wright's (1974)
88 mapping of the southern Alexander Hills (Tecopa) area, the description of his units (pCk1-
89 pCk4) do not closely match the descriptions in either Prave (1999) or Macdonald et al.
90 (2013). Reference to this unit is also made multiple times in Mrofka and Kennedy (2011),
91 who cite Wright (1974) as the primary source of this stratigraphic unit, and in Mahon et al.
92 (2014a) as a small channel-like feature at the top of KP3. Interestingly, Petterson et al. (2011)
93 do not refer to it in their summary paper of the western Death Valley stratigraphy.
94 Nevertheless, some authors have considered diamictites at the top of the Kingston Peak
95 (KP4) to have global age significance: Macdonald et al. (2013) attributed this unit to the
96 Marinoan glaciation. In the absence of good syn-depositional age constraints for the Kingston
97 Peak Formation (e.g. Vandyk et al., in review), it thus remains contentious whether diamictite
98 units are of local, regional, or global significance.

100 Macdonald et al. (2013) “observed” KP4 in the Saddle Peak Hills area, which they
101 considered to be laterally equivalent to the Wildrose Diamictite in the Panamint Range (c.f.
102 Prave, 1999, who considered this equivalent to KP2/3). The crux of the issue is that there is
103 no formally documented type section or type area for the KP4 stratigraphic unit, yet in spite
104 of this, it has been argued that the unit could be used for correlation across the North
105 American Cordillera: Macdonald et al. (2013) attributed it to the Marinoan glaciation. With
106 Macdonald et al. (2013) proposing that the lowermost unit of the Kingston Peak Formation
107 (KP1 sensu Prave, 1999) was genetically unrelated to glaciation, Le Heron et al. (2017)
108 questioned the applicability of this regional scale stratigraphy for the Silurian Hills area,
109 because at least four distinct diamictite-dominated intervals can be observed in 1.4 km of
110 stratigraphy (rather than the two recognised by Macdonald et al., 2013: i.e. KP2 and KP4). Le
111 Heron et al. (2017) thus raised the possibility that Cryogenian glaciation in the Death Valley
112 area may have been diachronous from outcrop belt to outcrop belt. This is an uncomfortable
113 proposal because it conflicts with the idea of using diamictites as time markers over wide
114 areas. In their provenance study, Mahon et al. (2014b) were able to distinguish different
115 detrital zircon suites for the Pahrump Group, and for the Kingston Peak Formation where
116 sediment input from the north, south, west and east was proposed. A progressive unroofing
117 process was proposed, but the resolution of the published data do not enable the idea of a
118 major break in time (i.e. major unconformity) between KP3 and KP4 to be substantiated. This
119 idea awaits further data and further research.

120 Noting the problems above, we have two objectives, namely (i) to provide the first
121 complete description of the thickest diamictite-bearing interval in the Death Valley area (S
122 Kingston Range) and (ii) to propose new interpretations and palaeogeographic context for the
123 diamictites. Building on recent work which focused on a limited interval of dropstone-
124 bearing strata (Le Heron and Busfield, 2016), the new data in this paper are extremely
125 important for evaluating regional correlations and evaluating temporal changes in Cryogenian
126 glacial environments. Furthermore, the descriptions and interpretations are vital in providing
127 (i) new data on a candidate region for placing a Cryogenian GSSP and (ii) properly
128 evaluating the origins of the diamictites, and (iii) using sedimentological and stratigraphic
129 relationships to consider the regional vs global significance of glacial cycles within the
130 succession.

131 The tectonostratigraphic framework of Macdonald et al. (2013) was proposed on the
132 basis of mapping work in the Kingston Range and in the Saddle Peak Hills (**Fig. 1**). Both
133 areas were mapped by students to enable a composite stratigraphic framework that refined the
134 previous work of Prave (1999). Further west in the Panamint Range, more continuous
135 succession of strata is preserved including a laterally extensive limestone interval interpreted
136 as a possible cap carbonate (the Sourdough Limestone) at the top of the interpreted Sturtian
137 succession (Prave, 1999). However, detailed sedimentological investigation in that area is
138 made all the more difficult as a result of the high grade (amphibolite) metamorphic overprint
139 (Pettersen et al., 2011). In our study area, the southern Kingston Range, the upper part of the
140 KPF is truncated, at a very low angle, by the Noonday Dolomite. This dolomite unit contains
141 a stable C isotope signature comparable to that of post-Marinoan cap carbonates (Prave,
142 1999; Macdonald et al., 2013). Whilst detailed studies of the Noonday Formation in the
143 southern Kingston Range have yet to be done, recent work in the Saddle Peak Hills area by
144 Creveling et al. (2016) established a full carbonate platform facies model. In that study, a
145 basal unit with dololaminites was found to be typical, with tube-like structures once thought to
146 be stromatolitic and now interpreted as gas-escape structures (Creveling et al., 2016) are
147 recognised.

148

149 **3. The southern Kingston Range succession**

150 *3.1 Introduction*

151 The southern Kingston Range, which was first mapped by Calzia et al. (1987), exposes the
152 geographically widest outcrop belt of Kingston Peak Formation (KPF) strata in the range and
153 also the thickest strata (**Fig. 1**). Dip angles are typically greatest nearest to the Kingston
154 Range granite intrusion at the western margin of the outcrop belt. In the Kingston Range, the
155 Beck Spring Dolomite forms the basal Pahrup Group outcrop, overlain by a recessive unit
156 comprising siltstone-sandstone intercalations interpreted as the lowermost, non-glacial strata
157 of the KPF (KP1 of Prave, 1999). A poorly exposed example of the diamictite facies
158 association of Le Heron et al. (2014), traditionally interpreted as unit KP2 (Prave, 1999;
159 Macdonald et al., 2013), crops out above. This basal diamictite can be followed along strike
160 and it is very well exposed 7 km further north, where it is intercalated with dropstone-bearing
161 strata (Le Heron et al., 2014). This is overlain by the megaclast facies association, interpreted
162 as an olistostrome, containing up to 700 m-scale blocks of the Beck Spring Dolomite.

163 3.2 Methodology

164 Over 6 weeks from 2014-2015, we measured a 2.5 km thick composite section (Fig. 2) of the
165 KPF in the southern Kingston Range. This is the thickest KPF section in the entire Death
166 Valley region. In this area, the following general stratigraphic summary can be made. The
167 basal (KP2: Prave, 1999) diamictite is overlain by a thick, chaotically organised olistostrome
168 complex. This in turn is capped by better organised graded conglomerate and sandstone beds
169 that were briefly described and interpreted by Le Heron and Busfield (2016). These in turn
170 pass upwards into a hitherto undescribed, but very well exposed, diamictite that is
171 intercalated with graded conglomerate, sandstone and mudstone (**Fig. 2**). Our study used both
172 mapping (basal diamictite and olistostrome complex), and logging at dm-scale resolution
173 (supra-olistostrome complex) to derive the 2.5 km thickness (the olistostrome contains no
174 definite *in situ* bedding planes). Previously, Mrofka and Kennedy (2011) reported that the
175 succession was 3.2 km thick in this area (see their Figure 40.2 “Horsethief Mine section”).
176 Their estimation is ~0.7 km thicker than ours, possibly because rotated sandstone beds within
177 the olistostrome were used for trigonometric calculations to determine true thickness of this
178 unit.

179 In this paper, we build on the sedimentological template developed for other outcrop
180 belts of the KPF by Le Heron et al. (2014), Le Heron and Busfield (2016) and Busfield and
181 Le Heron (2016). These studies emphasise the co-genetic development of turbidites and ice-
182 contact diamictites (Busfield and Le Heron, 2016). These studies established a suite of *facies*
183 *associations* reflecting the dominant signature of gravity flows, with the full spectrum of
184 debrites to low density turbidites recognised. Two of these deserve special emphasis: (i) a
185 megaclast facies association (interpreted as km-scale blocks emplaced as part of an
186 olistostrome) and (v) a diamictite facies association (interpreted as a series of glaciogenic
187 debris flows, i.e. material reworked by gravity flows that is ultimately of glacial origin). The
188 Kingston Range is viewed as a proglacial basin (Le Heron et al., 2014): it lacks
189 glacitectonized deposits that are locally represented in Sperry Wash some 50 km to the east
190 (Busfield and Le Heron 2016). Rather than focus on the sedimentological minutiae, the
191 present manuscript is directed at considering the stratigraphic significance of diamictites in
192 this important section.

193

194 3.3 Olistostrome complex: description

195 The metabasite suite comprises blue-green weathering crystalline rocks with
196 intercalated sedimentary rocks. Both volcanic ash (Calzia et al., 1987) and fragments of
197 diabase from the Crystal Springs Formation (Calzia et al., 2000) have been reported from the
198 KPF previously: we discovered a 350 m thick diabase body (**Fig. 2**). A panoramic perspective
199 (**Fig. 3**) highlights the internal heterogeneity of the olistostrome complex (**Fig. 3**), which
200 includes large blocks of carbonate and arkose. The olistostrome complex commences with a
201 single block of dolostone (**Fig. 2, Fig. 3**) which has intensely boudinaged (**Fig. 4 A**) and
202 folded (**Fig. 4 B**) a mixed carbonate-siliciclastic interval beneath it. Solitary blocks of
203 diamictite are encased within the olistostrome complex, and these can be demonstrated to be
204 allochthonous on account of their locally oversteepened dips.

205 Outcrops typically include bulbous masses of material that are devoid of any internal
206 fabric or foliation (**Fig. 4 C**). Elsewhere, xenoliths of sandstone and dolostone (**Fig. 4 D**) are
207 observed. These are typically highly irregular in outline and exhibit baked margins.
208 Elsewhere, ovoid “clast” and groundmass relationships are only faintly recognisable in the
209 metabasite (**Fig. 4 E**). Petrographic analysis reveals extensive chloritization and alteration of
210 the protolith, with chlorite laths possibly pseudomorphing feldspar (**Fig. 4 F**). At the outcrop
211 scale, the metabasite rocks are intercalated with both normally and inversely graded
212 siliciclastic sedimentary rocks that are essentially identical to those in the supra-olistostrome
213 strata. The contact between the metabasite and the normally graded sedimentary rocks is
214 concordant and devoid of a baked margin. Unidirectional ripple marks (**Fig. 4H**) are recorded
215 on the upper surface of normally-graded sandstones.

216

217 *3.4 Olistostrome complex: interpretation*

218 The occurrence of an olistostrome, originally mapped in the Kingston Range as a
219 “megabreccia”, has long been known (Hewett, 1956). The present study area was explored in
220 terms of its resource potential by Calzia et al. (1987), noting the occurrence of iron
221 accumulations both as sedimentary units within the KPF, and as skarns in contact with the
222 Kingston Peak granite. These authors did not discuss the presence of metabasites within the
223 olistostrome complex. Elsewhere in the Kingston Range (in the Excelsior Mine area, ~12 km
224 NW of our study area) a 1.08 Ga diabase intrudes the Crystal Spring Formation (Heaman and
225 Grotzinger, 1992). There are two possibilities: (i) extrusion of lava flows during rifting
226 followed by downslope mobilisation and incorporation into the olistostrome (e.g. in the Moni

227 Mélange, Cyprus: Robertson, 1977) or (ii) that the metabasites are simply remobilised
228 fragments of the Crystal Spring Formation diabase. The latter interpretation is supported on
229 the basis of U-Pb dates obtained from apatites (Vandyk et al., in review). The occurrence of
230 both normally and inversely graded sedimentary rocks together is noteworthy, because these
231 facies (interpreted as turbidites and debrites respectively) have closely comparable
232 counterparts in the supra-olistostrome succession as we shall discuss below.

233

234 *3.5 Supra-olistostrome strata: description*

235 The succession immediately above the olistostrome was described by Le Heron and Busfield
236 (2016). That paper documented a well exposed interval of approximately 187 m thick, which
237 was investigated in spring 2014. Subsequently, a 2015 field season included the discovery of
238 excellent, complete sections above the olistostrome to be documented through the entirety of
239 the uppermost KPF to the contact with the overlying Noonday Dolomite: an additional 430 m
240 of superbly exposed strata allowing us to include a composite, though almost continuous,
241 high resolution section through 617 m of stratigraphy (**Fig. 5**). The lowermost 180 m or so of
242 supra-olistostrome strata is dominated by alternating packages of interbedded heterolithic and
243 lonestone-bearing facies associations, punctuated at intervals by occurrences of the pebble to
244 boulder conglomerate association. Le Heron and Busfield (2016) interpreted the interbedded
245 heterolithic facies association - which comprises intercalated normally graded beds, ripple
246 cross-laminated intervals and clast-free mudrocks - as low-density turbidites. A similar
247 interpretation for the lonestone-bearing facies association was proposed, with the key
248 difference lying in the occurrence of abundant dropstones. Hence, a strong overprint of ice-
249 rafting was proposed, and hence evidence for a glacial influence, in some intervals of the
250 supra-olistostrome strata. The pebble to boulder-conglomerate facies association, by
251 comparison, was interpreted as high-density turbidite deposits. No diamictites were described
252 by Le Heron and Busfield (2016).

253 Appraising the entirety of the supra-olistostrome succession (**Fig. 5**), three first-order
254 generalisations can be made: (1) the occurrence of thicker, progressively more amalgamated
255 packages (~50 m or so) of the pebble to boulder conglomerate association upsection, (2) the
256 intercalation of the interbedded heterolithic facies association between the conglomerates and
257 (3) the appearance of muddy diamictites in the succession, initially as isolated beds at 180 m
258 and 198 m, and forming repeated, progressively thicker (~30 m) beds/units over an interval of

259 almost 100 m (between 509 m and 608 m on the measured section **Fig. 5**) at the very top of
260 the KPF. In this paper, we refer to this interval as the upper diamictite. Establishing the
261 correct stratigraphic context of the upper diamictite, and its relationship to underlying
262 deposits, is vital seeing that it is viewed as the Cordilleran equivalent of the Marinoan glacial
263 record (Macdonald et al., 2013). The diamictite beds show an interesting relationship with
264 other siliciclastic deposits. For example, a clear coarsening-up motif can be identified from
265 509-547 m; the lower part of this section comprises coarsening upward diamictite (showing
266 both increase in clast size and matrix composition tending toward more sandy) whereas the
267 upper part comprises stacked, normally graded granule-pebble and cobble-boulder
268 conglomerates (**Fig. 5**). In other occurrences beneath the Noonday dolomite, abundant
269 dropstones are recorded within stratified diamictites, particularly in the interval at 582-588 m
270 and directly below the Noonday (604-607 m). Normally graded conglomerates and
271 sandstones account for any non-diamictite strata in the upper part of the KPF. Palaeocurrent
272 data (shown next to the log in position and as summary rose diagrams) indicate a uniform SE
273 palaeoslope throughout deposition, with very few exceptions. Thus, there is no apparent
274 difference in flow direction recorded below or within the upper diamictite interval.

275 Owing to its stratigraphic position almost 2 km above the basal diamictite (KP2 of
276 Prave, 1999: **Fig. 2**), it is important to consider the origin of the upper diamictite separately.
277 Whilst sedimentary evidence for a glaciogenic origin for the basal diamictite was well
278 established in the northern part of the Kingston Range (intercalated mudrocks bear
279 dropstones: Le Heron et al., 2014), the sedimentological case for a glacial origin in the upper
280 diamictite (KP4 of Prave, 1999) remains to be fully established, although it should be noted
281 that Mrofka (2010) recovered some excellent striated pebbles from this level in the Jupiter
282 Mine area, some 8 km north. The gradational relationship between diamictite lithofacies and
283 normally graded sandstone beds in the upper diamictite interval is apparent (**Fig. 6 A, B**).
284 Cobble-sized dropstones occur within stratified diamictites (**Fig. 6 B**), and some of these
285 exhibit striated surfaces (**Fig. 6 C**). Dropstones are abundant at the pebble-scale and rather
286 than deflect / downwarp the diamictite lamination, the stones puncture into underlying
287 laminae and are draped by undeformed laminae (**Fig. 6 D, E**). The dropstones occur at
288 intervals throughout the upper diamictite, including immediately below the contact with the
289 Noonday Dolomite (**Fig. 6 F**).

290 The upper diamictite interval contains numerous examples of asymmetric rippled
291 surfaces (**Fig. 7 A**), pointing to unidirectional flow into the basin. It also contains excellent

292 examples of normally graded beds (**Fig. 7 B, C**) which are compositionally and texturally
293 identical to those described previously from the lower levels of the supra-olistostrome strata
294 (Le Heron and Busfield, 2016) and indeed to those contained within the olistostrome complex
295 (see **Fig. 4 G**). Diamictite beds show upward transitions into normally-graded conglomerate
296 (**Fig. 7 D**); in other cases stacked, intervals dominated by normally-graded beds are
297 punctuated by occasional diamictite beds (**Fig. 7 E**). Unidirectional ripple cross-lamination,
298 almost exclusively indicating a SE-palaeoflow, occurs at the top of many normally-graded
299 beds. The diamictites vary widely in terms of colour (including both reddish-brown (**Fig. 8**
300 **A**) and green (**Fig. 8 B**) varieties), in terms of the number of clasts, and in terms of clast
301 composition. Clasts include psammite (**Fig. 8 D**), dolostone (**Fig. 8 E**), metabasite (**Fig. 8 E**,
302 **F**), oncolitic dolostone (**Fig. 8 G**), stromatolitic dolostone, sandstone and quartzite (**Fig. 8 H**),
303 together with schists.

304

305 *3.6 Supra-olistostrome strata: interpretation*

306 The supra-olistostrome package is interpreted to record the progradation of a major
307 subaqueous fan complex directly comparable to that in the Sperry Wash area some 50 km to
308 the west (Busfield and Le Heron, 2016). The overall coarsening upward trend is compatible
309 with progressive infill of the basin, with the abundant stacked fining up motifs both in the
310 pebble to boulder conglomerate and interbedded heterolithic facies associations interpreted as
311 a spectrum of high- to low-density turbidites. The diamictite facies association, which occurs
312 at an almost identical stratigraphic level to that at Sperry Wash (Busfield and Le Heron,
313 2016), is interpreted as a combination of primary and secondary glacial deposition, including
314 both primary rain-out sedimentation, and downslope reworking and modification of the
315 glacial debris. The clear vertical transitions that can be observed, at an outcrop scale, between
316 diamictite and sandstone (**Fig. 6 A**) or diamictite and conglomerate (**Fig. 7 D**) strongly imply
317 a genetic (process) connection between these lithologies. The massive diamictites are
318 interpreted as debrites, representing reworked equivalents of the stratified diamictites. A
319 direct glacial influence for the stratified diamictites is implied by (i) the abundant dropstone
320 textures within these facies and (ii) the striated surfaces of some clasts. The occurrence of a
321 wide variety of extra-basinal clasts (igneous and metamorphic lithologies) within the
322 diamictites is strongly suggestive of a wide provenance compatible with the re-advance of ice
323 masses over the Southern Kingston Range.

324 The relationships between diamictites and associated facies have been poorly
325 documented to date. In the southern Kingston Range, high quality exposure demonstrates the
326 intercalation of diamictites, conglomerates (as noted above), and thin heterolithic intervals
327 (**Fig. 9**). In previous work (Le Heron et al., 2014), it was suggested that the Basal Diamictite
328 of the KPF (i.e. those belonging to unit KP2 of Prave, 1999) (**Fig. 2**) represents mostly
329 glaciogenic debris flow deposits, with some evidence for stratification testifying to waterlain
330 deposition. For the upper diamictite, we propose a similar model, albeit with a small but
331 important modification. As established above, a genetic connection between diamictites and
332 conglomerates is indicated by the transitional nature of boundaries, some of which are diffuse
333 (e.g. **Fig. 7 D**). Stratification is also represented in these diamictites, but importantly, we
334 recognise both striated clasts (**Fig. 6 C**) and the piercement of stratification by outsized clasts
335 at some parts of the diamictite exposure (**Fig. 6 E**). These latter observations demonstrate
336 that the clasts represent ice-rafted debris (Le Heron, 2015).

337

338 **4. Lateral extent and significance of diamictites and associated strata**

339 The authors completed two closely spaced transects (separated by < 1km) throughout the
340 supra-olistostrome succession in 2015. The thickest (and southernmost) of these is
341 incorporated into our representative stratigraphic column (**Fig. 2**) and has been presented in
342 detail as **Fig. 5**. A similarly detailed (northern) section was completed for comparative
343 purposes, and an attempt to correlate these two sections is made herein (**Fig. 9**). In many
344 cases, beds and bedsets can be traced out on foot along strike. On the correlation, an obvious
345 thick conglomeratic package (commencing at about 275 m) is immediately overlain by the
346 upper diamictite in both logs. The basal contact of this conglomerate package is undulatory in
347 character, cutting down into underlying beds to produce a relief of at least 5 m. It is
348 dominated by (i) abundant large boulders (>1 m diameter) and (ii) a wide variety of
349 lithologies (psammite, dolostone, metabasite, oncolitic dolostone, stromatolitic dolostone,
350 sandstone, quartzite and schist). Below the thick conglomerate package, possible channel
351 geometries are apparent between the interbedded heterolithics and pebble to boulder
352 conglomerate facies associations, pinching out from log 1 to log 2 (**Fig. 9**), and toplap and
353 truncation occurs beneath at least one of these conglomeratic bedsets.

354 Diamictites at the top of the KPF in the northern and central Kingston Range (KP4 of
355 Prave, 1999) are well established (e.g. Mrofka, 2010; Mrofka et al., 2011; Macdonald et al.,

2013), though comparatively little described. Occurrences of conglomerate within the upper diamictite package are identical in motif to their counterparts below the thick conglomerate package (typically exhibiting normal grading) but are encased above and below by the diamictite facies association. The conglomerates form part of repetitive fining upward cycles at the bed scale, with typical upward trends over a bed from massive conglomerate, through diffusely laminated intervals to cross-laminated, medium-grained sandstone. Lensoid geometries for the pebble to boulder conglomerate and interbedded heterolithic intervals are observed, and in at least one case (437 m, log 1) lateral transition from conglomerate to heterolithic deposits can be demonstrated.

365

366 **5. The Kingston Range Fan**

367 Le Heron et al. (2014) and Le Heron and Busfield, (2016) proposed that the supra-olistostrome succession accumulated in a basin that was dominated by turbidite and debrite delivery. The occurrence of dropstones both in fine-grained facies toward the base of the supra-olistostrome succession and in diamictites at its top, testifies to a strong glacial influence (and possibly control upon) stratigraphic architecture. Here, we propose that the overall coarsening upward profile of the supra-olistostrome succession corresponds to the progradation of a sand-rich subaqueous fan as defined by Reading and Richards (1994) and which we term the Kingston Range Fan.

375 The stacked coarsening upward cycles >50 m thick are interpreted as stacked fan lobes, with the abrupt transition into mudrocks at the top of these cycles representing local fan lobe or fan lobe element abandonment (Macdonald et al., 2011; Pyles et al., 2014). The intercalation of graded conglomerates, with thick and continuous sections of the sheet heterolithics facies association, testifies to the development of a fan that dominantly accumulated via a spectrum of high to low density turbidity currents. The thick conglomeratic package with internal scours immediately below the upper diamictite is interpreted as a series of proximal stacked channels deposited by high density turbidites. Even if the recognition of individual fan lobes is not always clear cut (Prélat and Hodgson, 2013), the stratigraphic position of the thick conglomerate package on top of a well expressed, >400 m thick coarsening upward succession shows clear comparison to ancient outcrop examples of submarine fans in Ireland (Pyles et al., 2014).

387 Interestingly, the lonestone bearing facies association- toward the base of the fan as
388 described by Le Heron and Busfield (2016)- does not occur in the upper part of the fan (upper
389 350 m of the KPF). Nevertheless, its presence implies the (re)establishment of a glacial
390 influence on deposition early on in fan development, as recorded in comparatively distal
391 turbidites with dropstones. We posit that the stratified diamictite may be the proximal
392 equivalent of the dropstone-bearing heterolithics of the lonestone facies association, thus
393 explaining (i) the upsection disappearance of the lonestone-bearing facies associations to be
394 replaced by (ii) the upper diamictite at the top of the fan.

395 It is proposed that the upper diamictite is genetically related to underlying deposits,
396 thus demonstrating that the Kingston Range Fan developed either in response to, or under the
397 influence of, re-advancing ice masses. The intercalation of the diamictites with turbidites
398 highlights the genetic connection. Based on this, we do not strongly endorse the idea that in
399 the Southern Kingston Range, and perhaps throughout the eastern Death Valley area more
400 generally, unit KP3 represents the upper part of a Sturtian signal, and the unit KP4 (=upper
401 diamictite of this study) represents a Marinoan glacial phase (see Macdonald et al., 2013).
402 The only possible candidate for an unconformity- an undulating contact of the boulder
403 conglomerate package just below the upper diamictite (**Fig. 9**) - is interpreted as a series of
404 proximal stacked channels on the upper part (i.e. proximal reaches) of the Kingston Range
405 Fan. The reappearance of turbidite beds immediately above the boulder conglomerate
406 package (**Fig. 7 B, C**) underscores its relationship to the fan system beneath: once the boulder
407 conglomerate package was emplaced, normal sedimentation conditions resumed, culminating
408 in deposition of the upper diamictite.

409 In summary, based upon our field observations in the thickest succession of the KPF,
410 we propose that there is a genetic connection between the supra-olistostrome complex and the
411 upper diamictite, in the eastern Death Valley area. This interpretation contrasts with previous
412 views that the upper diamictite (KP4 of Prave, 1999) represents the deposits of a separate,
413 possibly Marinoan glaciation, as argued by Macdonald et al. (2013). It should be appreciated
414 that absolute age constraints on the KPF remain poor. Assuming that the C isotope profile in
415 the Noonday Dolomite faithfully records a post-Marinoan signal (Prave, 1999), our
416 observations to not discount the possibility that the Kingston Range had become a palaeohigh
417 during the Marinoan glaciation, with no sediments being deposited. This study therefore
418 shows that detailed sedimentological observations have an important role to play in the
419 establishment of regional stratigraphic frameworks in the Neoproterozoic of the Death Valley

420 area, and across the Cordillera more generally. The recognition of a 2.5 km thick succession
421 that has a much more complete sedimentary record than previously assumed, is also
422 important in the context of the global search for a Cryogenian Global Stratotype Section and
423 Point (GSSP) (Condon et al., 2015).

424

425 **6. Representativeness, completeness, and sequence stratigraphy**

426 In the southern Kingston Range, the thickest hitherto described section of the Kingston Peak
427 Formation raises questions about representativeness and completeness of Cryogenian glacial
428 strata. In the recent paper, Le Heron et al. (2017) presented new data from the Silurian Hills-
429 approximately 30 km west of the study area in the present paper- arguing, for the first time,
430 that clear evidence of glacial processes could be identified within the rock record. There,
431 previous workers (Basse, 1978) had proposed the occurrence of a major subaqueous fan
432 complex built from debrites and turbidites that resemble the strata in the supra-olistostrome
433 complex in the southern Kingston Range. Those diamictites, and associated dropstone-
434 bearing heterolithics, were dominated by basement-derived clasts (including gneiss, schist,
435 granitoid and quartzite).

436 In a similar manner to the Kingston Range succession, megaclasts of carbonate were
437 also recognised, and interpreted as up to four intercalated olistostrome deposits. Le Heron et
438 al. (2017) pointed out the problems with establishing the significance of the multiple
439 stratigraphic occurrences of glacial diamictites in the Silurian Hills: do they represent
440 multiple phases of glacially sourced debrites from an ice margin during a single glacial cycle,
441 or do they represent multiple phases of advance and retreat? Considering the 1.4 km of KPF
442 stratigraphy in the Silurian Hills, the 2.5 km of KPF stratigraphy in the southern Kingston
443 Range, and the c. 1 km stratigraphy in the Panamint Range (see Miller, 1985; Prave, 1999;
444 Petterson et al., 2011), an abiding problem is in determining which of these differing, undated
445 sections should be regarded as the definitive Death Valley glacial record.

446 Much significance is placed on the “well-developed nonglacial stratigraphy” in the
447 Panamint Range (Macdonald et al., 2013, p. 1205), which includes a carbonate interval (the
448 Sourdough limestone). With the Sourdough limestone interpreted as a Sturtian cap carbonate
449 passing up into an interglacial / nonglacial stratigraphy, and the overlying Wildrose
450 Diamictite interpreted as a Marinoan glacial deposit (Prave, 1999; Petterson et al., 2011), it is

451 clear to see how this thinking has developed. Nevertheless, based on new work in the Silurian
452 Hills, we argue that a healthy degree of scepticism should be maintained. There, new U-Pb
453 apatite geochronology from metabasite bodies in the KPF yield 1.1 Ga dates (Vandyk et al.,
454 in review). These were previously interpreted as diabase sills, because the metabasite bodies
455 are bedding concordant and occur at multiple stratigraphic intervals. Close and careful
456 examination, however, reveals that the metabasites become disaggregated along strike, with
457 rounded boulders of the same metabasite material encased in glacial diamictite. Noting these
458 field relationships, the unexpectedly old U-Pb dates, and the geochemical similarity to
459 diabase sills in the underlying Crystal Spring Formation, Vandyk et al. (in review) proposed
460 that the diabase “sills” in the KPF were better interpreted as olistoliths. These authors also
461 recommended that given some geochemical similarities between the Silurian Hills
462 metabasites and so-called MORB pillow lavas in the Surprise Member of the KPF in the
463 Panamints (Hammond, 1983), their stratigraphic context should be rescrutinized (i.e. whether
464 they are *in situ* extrusives or whether they are also olistoliths). Similarly, given the km-size of
465 carbonate olistoliths across the Death Valley area (e.g. Walker et al., 1986; Prave, 1999;
466 Calzia et al., 2000; Macdonald et al., 2013; Le Heron et al., 2014; Le Heron et al., 2017), care
467 must be taken to ensure that carbonate intervals are really *in situ* beds and do not represent
468 olistoliths.

469 The above considerations suggest that the identification of a representative or
470 idealised glacial stratigraphy for the KPF over the Death Valley area is still premature.
471 However, based upon our comparative southern Kingston Range sections (**Fig. 9**), we
472 propose a sequence stratigraphic interpretation that follows the methodology of Powell and
473 Cooper (2002), and which has successfully been applied to Sturtian glacial strata in South
474 Australia (Busfield and Le Heron, 2014). This methodology can be used to unravel the nature
475 of glacial cycles, and by comparison to other outcrop belts, potentially enable common
476 stratigraphic patterns to be recognised. Based upon the stacking patterns of bedsets, we
477 identify some well-defined, progradational parasequence sets which collectively represent ice
478 minima, advance, retreat, and maximum systems tracts (**Fig. 9**). Some stratigraphic surfaces
479 are associated with truncation of underlying strata (e.g. glacial advance surface) whereas
480 other stratigraphic contacts (e.g. the glacial erosion surface) superpose the upper diamictite
481 succession on underlying heterolithics (**Fig. 9**). At the local scale, given the close spacing
482 between the detailed sections, (i) a case for ~50 m thick channels can be made and (ii) tolap
483 and truncation of beds beneath the glacial advance surface is notable. Collectively, these

484 phenomena testify to considerable lateral inhomogeneity within the succession at the local
485 scale. At the regional scale, they challenge us to consider which of the thick Death Valley
486 KPF successions is most representative of this formation at the local scale. In addition to the
487 clear role of tectonics superimposed on glaciation or vice-versa, this also applied to the fine-
488 grained record (e.g. shaley intervals in turbidites of the Kingston Range Fan): Trabucho-
489 Alexandre (2015) has argued that even for basinal shales there is more gap than stratigraphic
490 record. More widely, and at a global scale, we are challenged to consider which of the thick
491 Death Valley successions record the global signature of Sturtian glaciations, if there is indeed
492 a representative signature. These uncomfortable questions need to be addressed and
493 overcome in the search for a suitable Cryogenian GSSP.

494

495 7. Conclusions

- 496 • A complete, detailed section through the KPF in the southern Kingston Range is
497 presented for the first time. The true thickness measures 2.5 km, and represents the
498 thickest and arguably most complete section of this formation in the Death Valley
499 area. The succession comprises (i) a Basal Diamictite, (ii) an olistostrome complex,
500 including km-scale megablocks, succeeded by (iii) a supra-olistostrome succession
501 some 500 m thick;
- 502 • The supra-olistostrome succession includes 4 facies associations. The lowest 170 m is
503 dominated by intercalation of comparatively dilute (low density) turbidites (sheet
504 heterolithics), some of which contain abundant ice-rafted debris (lonestone-bearing
505 strata), and high density turbidites (cobble-to boulder conglomerate facies
506 association). Upsection, conglomerates become increasingly important, lonestone-
507 bearing heterolithics disappear, and a 100 m thick diamictite-dominated interval (the
508 upper diamictite) characterises the upper 100 m of the KPF. The overall coarsening
509 upward profile of the entire supra-olistostrome succession allows us to propose that
510 these rocks represent a subaqueous fan complex known herein as the Kingston Range
511 Fan;
- 512 • The intercalation of diamictites with turbidites in the upper diamictite interval
513 demonstrates a genetic relationship between diamictites and the Kingston Range Fan.
514 Gradation between stratified and massive diamictites (the former bearing dropstone
515 textures) suggests that the stratified diamictites were deposited directly through ice

516 rafting whereas the massive diamictites represent sediments reworked by debris flows.
517 The stratified diamictites are also posited to be proximal equivalents to the lonestone-
518 bearing facies association. Thus, there is no reason to argue that the upper diamictite
519 is the deposit of a separate glaciation from the remainder of the Kingston Range Fan
520 based on field relationships.

521 • Sequence stratigraphic analysis of the KPF identifies multiple systems tracts allied to
522 glacial advance, maxima, retreat and minima conditions in the southern Kingston
523 Range. Internal stratigraphic breaks are recognised that include glacial advance
524 surfaces, and a glacial erosion surface at the ice maxima. The former surface truncates
525 underlying strata which toplap against it, whilst the glacial erosion surfaces
526 superposes diamictite on top of underlying mass flows of the Kingston Range Fan. At
527 the local scale, dramatic lateral facies changes are also recognised, including
528 channels. Collectively, the inhomogeneity of the succession underscores the difficulty
529 in choosing the most characteristic Cryogenian succession, either as a faithful
530 representative of the KPF in Death Valley, or in a more global context as a
531 Cryogenian GSSP.

532

533 **Acknowledgments**

534 The authors are very grateful to the Geological Society of London for supporting our Death
535 Valley work via the Fermor Fund. In early stages of our work, we benefitted greatly from the
536 regional geological experience of Tony Prave, to whom we are very grateful for sending us
537 out to great localities and getting our ball rolling. We also acknowledge discussions with Jim
538 Calzia, Darrel Cowan, Marli Miller, Sammy Castonguay and Bennie Troxel on Pahrump
539 Group geology and stratigraphy in Death Valley, and thank Robert Mahon and Nicholas
540 Christie-Blick for helpful pre-reviews.

541

542 **References**

543 Basse, R.A., 1978, Stratigraphy, sedimentology, and depositional setting of the late
544 Precambrian Pahrump Group, Silurian Hills, California [M.S.thesis]: Stanford, California,
545 Stanford University, 86 p.

- 546 Busfield, M.E., Le Heron, D.P., 2014. Sequencing the Sturtian icehouse: dynamic ice
547 behaviour in South Australia. *Journal of the Geological Society of London* 171, 443–456.
- 548 Busfield, M.E., and Le Heron, D.P., 2016, A Neoproterozoic ice advance sequence, Sperry
549 Wash, California. *Sedimentology*. DOI: 10.1111/sed.12210
- 550 Calzia, J.P., Frisken, J.G., and Jachens, R.C., 1987, Mineral Resources of the Kingston Range
551 Wilderness Study Area, San Bernardino County, California. U.S. USGS Bulletin, 1709,
552 34pp.
- 553 Calzia, J.P., Troxel, B.W., Wright, L.A., Burchfiel, B.C., Davis, G.A., and McMackin, M.,
554 2000, Geologic map of the Kingston Range, southern Death Valley, California. USGC
555 Open-File Report 2000-412, 1 sheet.
- 556 Christie-Blick, N. 1982. Upper Proterozoic and Lower Cambrian rocks of the Sheeprock
557 Mountains, Utah: Regional correlation and significance. *Geological Society of America*
558 *Bulletin*, v. 93, p. 735-750.
- 559 Condon, D.J., Boggiani, P., Fike, D., Halverson, G.P., Kasemann, S., Knoll, A.H.
560 Macdonald, F.A., Prave, A.R., and Zhu, M., 2015, Accelerating Neoproterozoic research
561 through scientific drilling. *Scientific Drilling* v. 19, p. 17-25
- 562 Creveling, J.R., Bergmann, K.D., Grotzinger, J.P., 2016. Cap carbonate platform facies
563 model, Noonday Formation, SE California. *Geological Society of America Bulletin*, 128 (7-
564 8), 1249-1269.
- 565 Escutia, C., Eittreim, S.L., Cooper, A.K., and Nelson, C.H., 2000, Morphology and acoustic
566 character of the Antarctic Wilkes Land turbidite systems: icesheet- sourced versus river-
567 sourced fans. *Journal of Sedimentary Research*, v. 70, p. 84-93.
- 568 Hammond, J.L.G., 1983. Late Precambrian diabase intrusions in the southern Death Valley
569 region, California: Their petrology, geochemistry, and tectonic significance: (Ph.D.).
570 University of Southern California, United States - California.
- 571 Hazzard, J.C., 1933, Notes on the Cambrian rocks of the eastern Mohave Desert, California.
572 *California Univ. Pubs. Geol. Sci. Bull.*, v. 23, p. 57-70.

- 573 Heaman, L.M., and Grotzinger, J. P., 1992, 1.08 Ga diabase sills in the Pahrump Group,
574 California: Implications for development of the Cordilleran miogeocline. *Geology*, v. 20, p.
575 637-640.
- 576 Hewett, D.F., 1956, *Geology and mineral resources of the Ivanpah Quadrangle, California*
577 *and Nevada*. U.S. Geological Survey Professional Paper, v. 275, 172 pp.
- 578 Labotka, T.C., Albee, A.L., Lanphere, M.A., and McDowell, S.D., 1980, Stratigraphy,
579 structure and metamorphism in the central Panamint Mountains (Telescope Peak
580 quadrangle), Death Valley area, California, *Geological Society of America Bulletin*, 91,
581 843–933.
- 582 Le Heron, D.P., 2015, The significance of ice-rafted debris in Sturtian glacial successions.
583 *Sedimentary Geology*, v. 322, p. 19-33.
- 584 Le Heron, D.P., Busfield, M.E., and Prave, A.R., 2014a, Neoproterozoic ice sheets and
585 olistoliths: multiple glacial cycles in the Kingston Peak Formation, California. *Journal of*
586 *the Geological Society, London*, v. 171, p. 525-538.
- 587 Le Heron, D.P., Busfield, M.E., and Collins, A.S. 2014b, Bolla Bollana Boulder Beds: a
588 Neoproterozoic trough mouth fan in South Australia? *Sedimentology*, v. 61, p. 978–995.
- 589 Le Heron, D.P., and Busfield, M.E., 2016, Pulsed iceberg delivery driven by Sturtian ice
590 sheet dynamics: an example from Death Valley, California. *Sedimentology*, DOI:
591 10.1111/sed.12225
- 592 Le Heron, D.P., Tofaif, S., Vandyk, T., Ali, D.O. 2017. A diamictite dichotomy: Glacial
593 conveyor belts and olistostromes in the Neoproterozoic of Death Valley, California, USA.
594 *Geology*, 45, 31-34.
- 595 Link, P.K., Miller, J.M.G., and Christie-Blick, N., 1994, Glacial-marine facies in a
596 continental rift environment: Neoproterozoic rocks of the western United States
597 Cordillera. In: Deynoux, M., Miller, J.M.G., Domack, E.W., Eyles, N., Fairchild, I.J.,
598 Young, G.M. (Eds.), *Earth's Glacial Record*. Cambridge Univ. Press, Cambridge, 29– 46.

- 599 Macdonald, H.A., Peakall, J., Wignall, P.B., and Best, J., 2011, Sedimentation in deep-sea
600 lobe-elements: implications for the origin of thickening-upward sequences. *Journal of the*
601 *Geological Society of London*, v. 168, p. 319-331.
- 602 Macdonald, F.A., Prave, A.R., Petterson, R., Smith, E.F., Pruss, S.B., Oates, K., Trotsuk, D.,
603 and Fallick, A.E., 2013, The Laurentian record of Neoproterozoic glaciation, tectonism,
604 and eukaryotic evolution in Death Valley, California. *Geological Society of America*
605 *Bulletin*, v. 125, p. 1203-1223
- 606 Mahon, R.C., Dehler, C.M., Link, P.K., Karlstrom, K.E., and Gehrels, G.E., 2014a,
607 Geochronologic and stratigraphic constraints on the Mesoproterozoic and Neoproterozoic
608 Pahrump Group, Death Valley, California: A record of the assembly, stability, and
609 breakup of Rodinia. *Geological Society of America Bulletin*, v. 126, p. 652-664.
- 610 Mahon, R.C., Dehler, C.M., Link, P.K., Karlstrom, K.E., and Gehrels, G.E., 2014b, detrital
611 zircon provenance and paleogeography of the Pahrump Group and overlying strata, Death
612 Valley, California. *Precambrian Research*, v. 251, p. 102-117.
- 613 Miller, J.M.G., 1985, Glacial and syntectonic sedimentation: The upper Proterozoic Kingston
614 Peak Formation, southern Panamint Range, eastern California. *Geological Society of*
615 *America Bulletin*, v. 96, p. 1537-1553.
- 616 Mrofka, D., 2010, Competing models for the timing of Cryogenian Glaciation: Evidence
617 from the Kingston Peak Formation, southeastern California. PhD dissertation, University
618 of California, Riverside.
- 619 Mrofka, D., and Kennedy, M., 2011, The Kingston Peak Formation in the eastern Death
620 Valley region. In: *The Geological Record of Neoproterozoic Glaciations* (Eds E. Arnaud,
621 G.P. Halverson and G. Shields-Zhou). *Geological Society, London, Memoirs*, 36, 449-
622 458.
- 623 Partin, C.A, and Sadler, P.M. 2016. Slow net sediment accumulation sets snowball Earth
624 apart from all younger glacial episodes. *Geology*, doi: 10.1130/G38350.1
- 625 Petterson, R., Prave, A.R., and Wernicke, B.P., 2011, Glaciogenic and related strata of the
626 Neoproterozoic Kingston Peak Formation in the Panamint Range, Death Valley region,

- 627 California. In: The Geological Record of Neoproterozoic Glaciations (Eds E. Arnaud, G.P.
628 Halverson and G. Shields-Zhou). Geological Society, London, Memoirs, 36, 449-458.
- 629 Powell, R.D., Cooper, J.M., 2002. A glacial sequence stratigraphic model for temperate,
630 glaciated continental shelves. In: Dowdeswell, J.A., ÓCofaigh, C. (Eds.), Glacier
631 influenced Sedimentation on High-latitude Continental Margins. Geological Society of
632 London, Special Publications 203, pp. 214–244.
- 633 Prave, A.R., 1999, Two diamictites, two cap carbonates, two $\delta^{13}\text{C}$ excursions, two rifts: the
634 Neoproterozoic Kingston Peak Formation, Death Valley, California. *Geology*, v. 27, p.
635 339-324.
- 636 Prélat, A., and Hodgson, D.M., 2013, The full range of turbidite bed thickness patterns in
637 submarine lobes: controls and implications. *Journal of the Geological Society*, v. 170, p.
638 209-214.
- 639 Prélat, A., Covault, J.A., Hodgson, D.M., Fildani, A., and Flint, S.S., 2010, Intrinsic controls
640 on the range of volumes, morphologies, and dimensions of submarine lobes. *Sedimentary
641 Geology*, v. 232, p. 66-76.
- 642 Pyles, D.R., Strachan, L.J., and Jennette, D.C., 2014, Lateral juxtapositions of channel and
643 lobe elements in distributive submarine fans: Three-dimensional outcrop study of the Ross
644 Sandstone and geometric model. *Geosphere*, v. 10, p. 1104-1122.
- 645 Reading, H.G., and Richards, M., 1994, Turbidite Systems in Deep-Water Basin Margins
646 Classified by Grain Size and Feeder System. *AAPG Bulletin*, v. 78, p. 792-822.
- 647 Robertson, A.H.F. 1977. The Moni Mélange, Cyprus: an olistostrome formed at a destructive
648 plate margin. *Journal of the Geological Society*, London 133, 447-466.
- 649 Rooney, A.D., Strauss, J.V., Brandon, A.D., and Macdonald, F.A., 2015, A Cryogenian
650 chronology: Two long-lasting synchronous Neoproterozoic glaciations. *Geology*, v. 43, p.
651 459-462.
- 652 Shields-Zhou, G., Hill, A.C., and MacGabhann, B.A., 2012. Chapter 17: The Cryogenian
653 Period. In: Gradstein, F.M., Ogg, J.A., Schmitz, M. & Ogg, G. (eds), *The Geological Time
654 Scale 2012*, Elsevier B.V. p. 394-411.

- 655 Shields-Zhou, G.A., Porter, S., Halverson, G.P., 2016 A new rock-based definition for the
656 Cryogenian Period (circa 720-635 Ma). *Episodes* 39, 3-8.
- 657 Smith, A.G., Barry, T., Bown, P., Cope, J., Gale, A., Gibbard, P., Gregory, J., Hounslow, M.,
658 Kemp, D., Knox, R., Marshall, J., Oates, M., Rawson, P., Powell, J., Waters, C., 2015.
659 GSSPs, global stratigraphy and correlation. In: Smith, D.G., Bailey, R.J., Burgess, P.M.,
660 Fraser, A.J. (Eds), *Strata and Time: Probing the Gaps in Our Understanding*. Geological
661 Society, London, Special Publications 404, 37-67.
- 662 Spence, G.H., Le Heron, D.P., & Fairchild, I.J. 2016, Sedimentological perspectives on
663 climatic, atmospheric and environmental change in the Neoproterozoic Era.
664 *Sedimentology*, **63**, 253–306.
- 665 Taylor, J., Dowdeswell, J.A., Kenyon, N.H., and O’Cofaigh, C., 2002, Late Quaternary
666 architecture of trough-mouth fans: debris flows and suspended sediments on the
667 Norwegian margin. In: *Glacier-Influenced Sedimentation on High-Latitude Continental*
668 *Margins* (Eds J.A. Dowdeswell and C. O’Cofaigh), Geol. Soc. London Spec. Publ., v. 203,
669 p. 55–71.
- 670 Trabucho-Alexandre, J., 2015. More gaps than shale: erosion of mud and its effect on
671 preserved geochemical and palaeobiological signals. In: Smith, D.G., Bailey, R.J.,
672 Burgess, P.M., Fraser, A.J. (Eds), *Strata and Time: Probing the Gaps in Our*
673 *Understanding*. Geological Society, London, Special Publications 404, 251-270.
- 674 Vandyk, T.M., Chew, D.M., Thirlwall, M., Hennig, J., Manning, C.J., Knott, T., Tofaif, S.,
675 Ali, D.O., Busfield, M.E. (in review). Precambrian olistoliths masquerading as sills from
676 Death Valley, California. *Journal of the Geological Society*, London.
- 677 Walker, J.D., Klepacki, D.W., & Burchfiel, B.C. 1986. Late Precambrian tectonism in the
678 Kingston Range, southern California: *Geology*, 14, 15–18.
- 679 Wright, L.A. 1974. Geology of the southeast quarter of the Tecopa quadrangle, San
680 Bernardino and Inyo Counties, California [1:24,000]. Map sheet 20, California Division of
681 Mines and Geology.
- 682

683

684 **FIGURE CAPTIONS**

685 Figure. 1: Geological sketch map and location of sedimentary logs, samples, and photographs
686 in this paper, modified from Le Heron and Busfield (2016). A: Overview of the Death Valley
687 area, showing the location of the major mountain ranges that expose Neoproterozoic strata.
688 B: Geological sketch map of the area. Note that the main transects through the succession are
689 shown. The low-resolution and high-resolution transects together allow a sedimentary log
690 throughout the entire KPF to be presented (see Fig. 2). The two high resolution transects
691 through the supra-olistostrome strata includes an upper diamictite unit KP4 of Prave, 1999).
692 Transect (i), as the thickest and most complete of these, is shown on Fig. 5. The sedimentary
693 logs from both transects are compared and correlated on Fig. 9.

694 Figure. 2: Sedimentary log of the entire KPF exposed in the southern Kingston Range- the
695 thickest succession in the eastern Death Valley area. The authors undertook very detailed
696 measurement of the upper part of the succession (supra-olistostrome deposits) to a resolution
697 of 10 cm. Accurate portrayal of the olistostrome deposits was possible through mapping and
698 spot measurements, dip values, and true thickness restoration. Thus, the internal stratigraphy
699 of the olistostrome deposit is illustrated. The exposure quality of the basal diamictite (“KP2”)
700 is very low in the southern Kingston Range, so textural comparisons with the upper (“KP4”)
701 necessarily rely on observations made several kilometres north at 35°44.810N, 115°51.612W.

702 Figure. 3: Panoramic view (A= true scale; A'= 3 X vertical exaggeration) of the Kingston
703 Peak Formation in the southern Kingston Range from the lowermost strata (basal diamictite),
704 through the olistostrome complex (commencing in this location with a >500 m thick
705 dolostone block), the intercalated metabasites and turbidites, to the supra-olistostrome
706 succession represented by brownish weathering slopes toward the centre of the panoramic.
707 The panoramic spans about 110° from the left (NW) to right (E) of the image.

708 Figure. 4: Aspects of the olistostrome complex in the southern Kingston Range. A:
709 Boudinaged strata in the lowermost part of the olistostrome, immediately beneath the >500 m
710 thick dolostone megablock. B: Small-scale folds beneath boudinaged strata shown in A.
711 Images C-H show crystalline metabasites and associated sedimentary strata. C: Metabasite
712 and quartzite clasts sitting within a metabasite groundmass. D: Highly irregularly shaped
713 boulder of dolostone encased within metabasite groundmass. E: Pebble-sized clast of

714 metabasite in groundmass of the same composition, with subtle clast boundaries. F: Thin
715 section image of the metabasite, illustrating extensive chlorite replacement of feldspar. G:
716 Stratigraphic contact between metabasite and overlying siliciclastic sedimentary rocks:
717 concordant and conformable. H: Interference-rippled surface on a normally graded sandstone
718 sandwiched between metabasite deposits.

719 Figure. 5: Detailed logged section throughout more than 600 m of stratigraphy in the supra-
720 olistostrome interval in the southern Kingston Range. This detailed transect includes data
721 from two field seasons in 2014 and 2015. The lowest 170 m were logged in detail by Le
722 Heron and Busfield in 2014 (published in Le Heron and Busfield, 2016), with particular focus
723 on the distribution of ice-rafted debris. The overlying 430 m were logged in 2015, by Le
724 Heron, Ali and Tofaif, and are described in detail herein. All the data are considered in the
725 context of regional ice sheet dynamics in this paper, with particular focus on the context and
726 global significance of the diamictite facies association, commencing at 510 m. This has
727 previously been regarded as “Marinoan” in age, and genetically distinct as a unit from the
728 underlying strata (Macdonald et al., 2013).

729 Figure. 6: Diamictite lithofacies and stratigraphic contacts toward the top of the Kingston
730 Peak Formation. A: Vertical transition from massive, through stratified diamictite, passing up
731 into sandstone above the hammer handle. B: Cobble-sized dropstone (to the left of the
732 hammer) in stratified diamictite. Note graded sandstone beds above. C: Striated surface on a
733 sandstone clast embedded in massive diamictite. D and E: Small pebble-sized dolostone
734 clasts in stratified diamictites. In each case, laminations are punctured beneath the clasts. F:
735 Upper contact between stratified diamictites of the Kingston Peak Formation and the
736 Noonday Dolomite. Strata are dipping at about 45°, and the base of the Noonday is a low
737 angle, but demonstrably angular, unconformity. Whilst the contact between the formations
738 appears conformable at a local scale, tracing the contact for a few hundred metres along strike
739 provides evidence for truncation of diamictite beds.

740 Figure. 7: Features diagnostic of turbidites in the uppermost part of the Kingston Peak
741 Formation. A: Asymmetric ripples on the surface of a sandstone bed, indicative of a
742 palaeoflow moving in the direction implied by the arrow (i.e. toward the SE). B: Relationship
743 between rippled surface shown in A and overlying deposits. The rippled sandstone surface is
744 directly overlain by highly recessive mudstone (covered in vegetation) and then a graded bed
745 on which the hammer is placed. C: orthogonal view of the graded bed shown in B. Note the

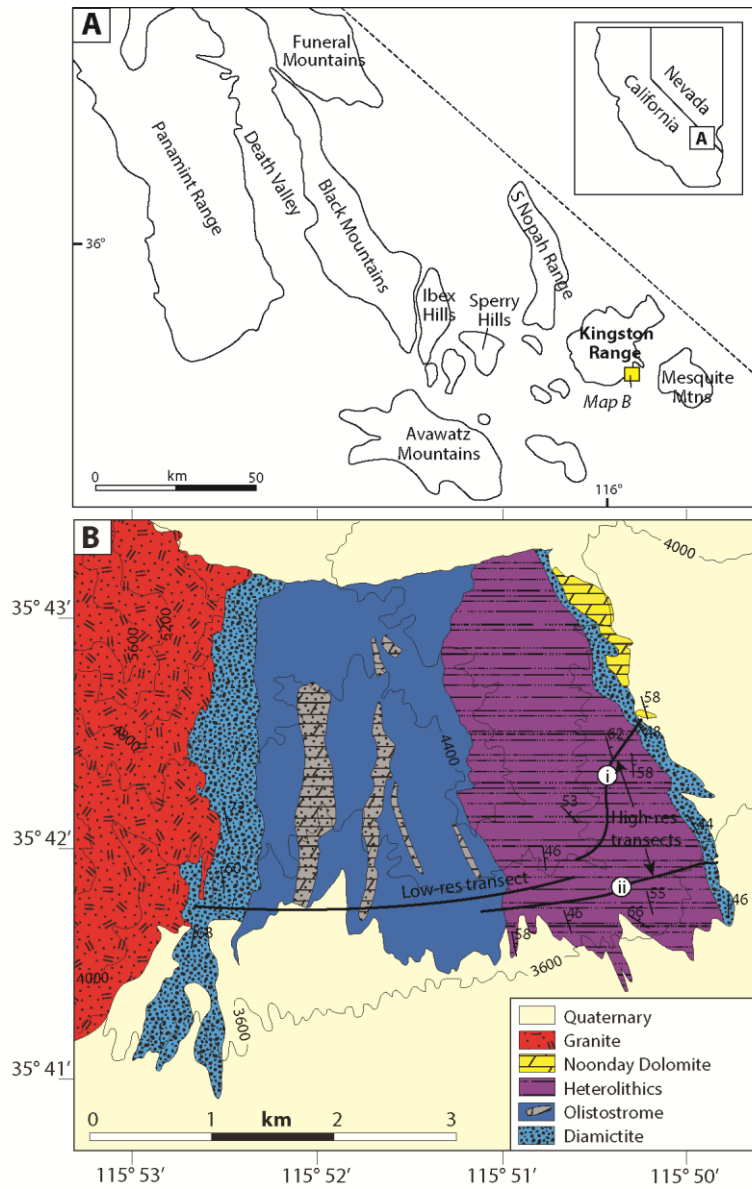
746 clear vertical transition from clast-supported conglomerate to reddish-brown sandstone. D:
747 Relationship between diamictite and normally graded conglomerate: transitional. E:
748 Repetitively stacked graded beds, interrupted by a massive diamictite bed. Note the
749 concordant though slightly irregular contact. F: Detail of unidirectional cross-lamination
750 toward the top of one of the sandstone beds shown in E.

751 Figure. 8: Textures and composition of the upper diamictites of the Kingston Peak Formation.
752 A and B: Ferric and ferrous variants of stratified diamictite. C to H: examples of pebble-sized
753 clasts. C and D show predominantly dolostone clasts, though D shows a metamorphosed
754 sandstone clast (psammite). E and F show finely crystalline and coarsely crystalline variants
755 of a metabasite that has identical weathering properties to the metabasites in the olistostrome
756 complex. The clasts are thus considered to be locally sourced. G: Oncolitic dolostone,
757 possibly derived from the Beck Spring Formation. H: sandstone and quartzite clasts.

758 Figure. 9: Two closely spaced sedimentary logs through the uppermost part of the Kingston
759 Peak Formation (2015 traverse), with an attempted correlation between them. The upper 430
760 m of Fig. 3 corresponds to the log shown on the left. Note evidence for (a) impressive lateral
761 thinning of conglomerates between 110-155 m on log I and log ii; (b) possible truncation and
762 toplap at 225 m; (c) internal heterogeneity within the upper diamictite. A sequence
763 stratigraphic analysis, based on the methodology of Powell and Cooper (2002) and successful
764 applied elsewhere to Cryogenian diamictite successions (Busfield and Le Heron, 2014) is
765 shown to the right of the sections.

766

767



768

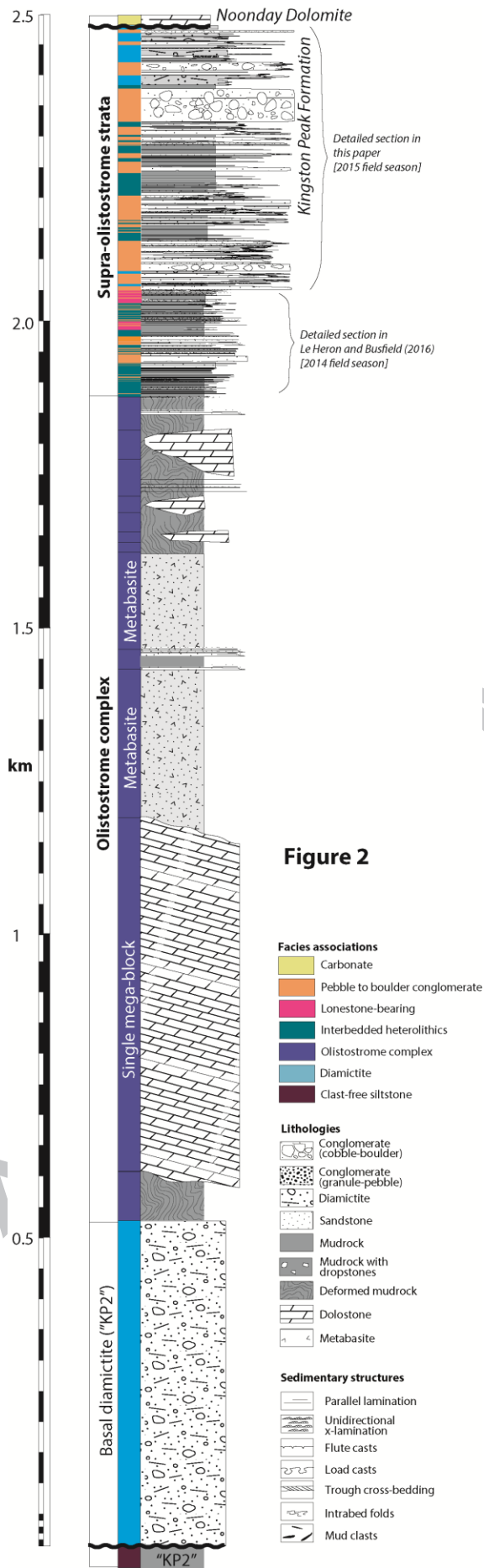
769

770

771

772

773



MANUSCRIPT

775



Figure 3

776

777

778

779

780

781

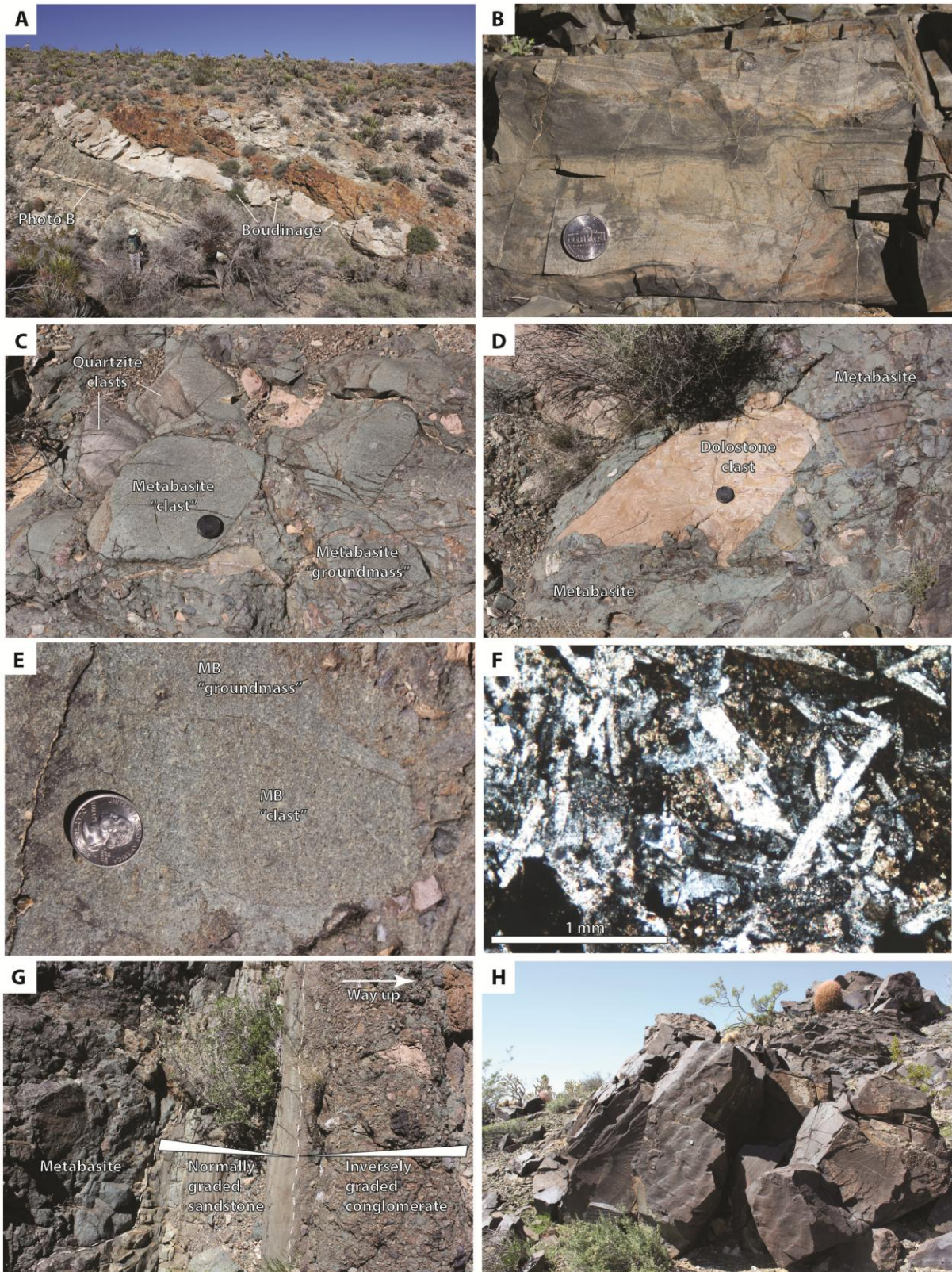
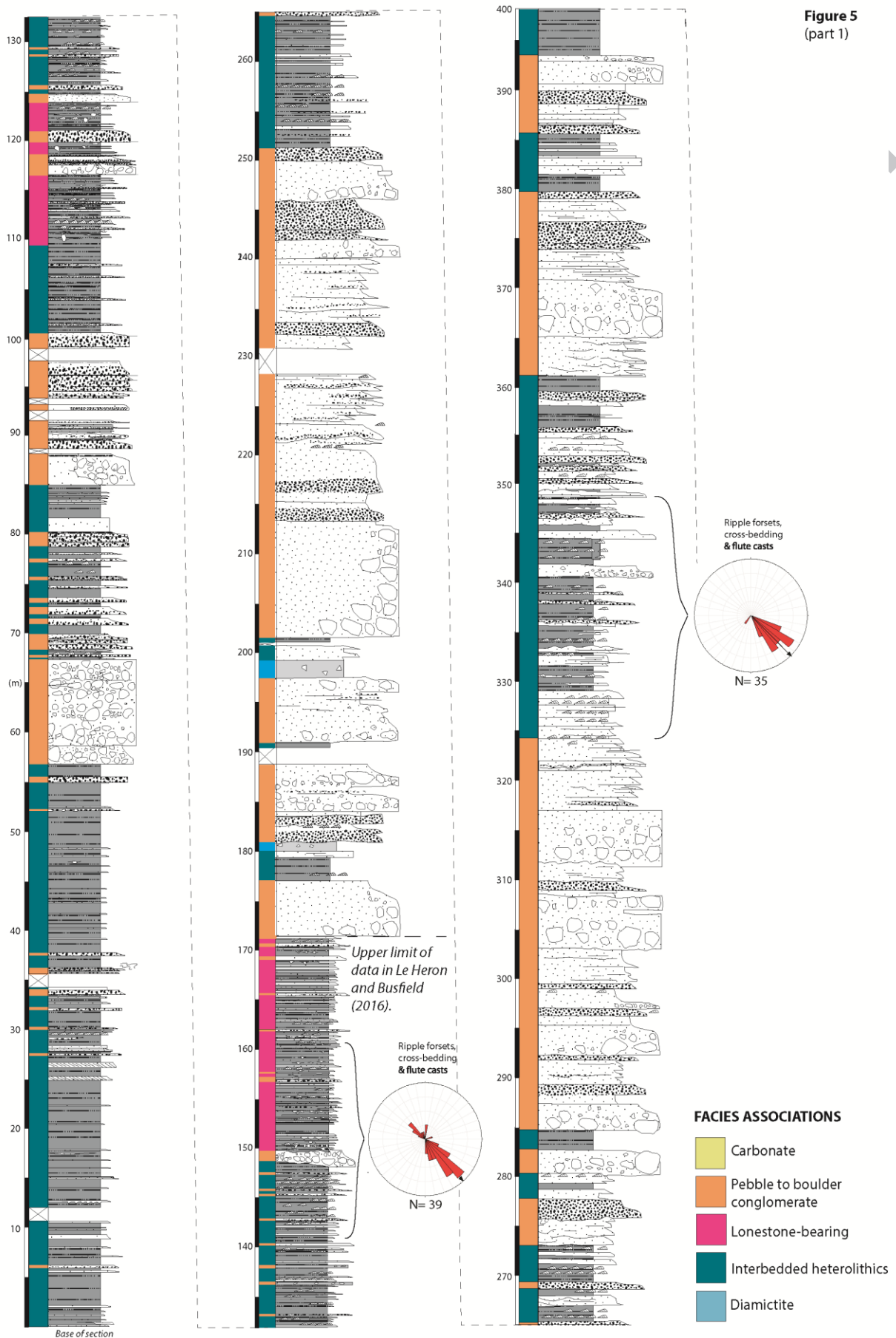


Figure 4

782

783

784



SCRIPT

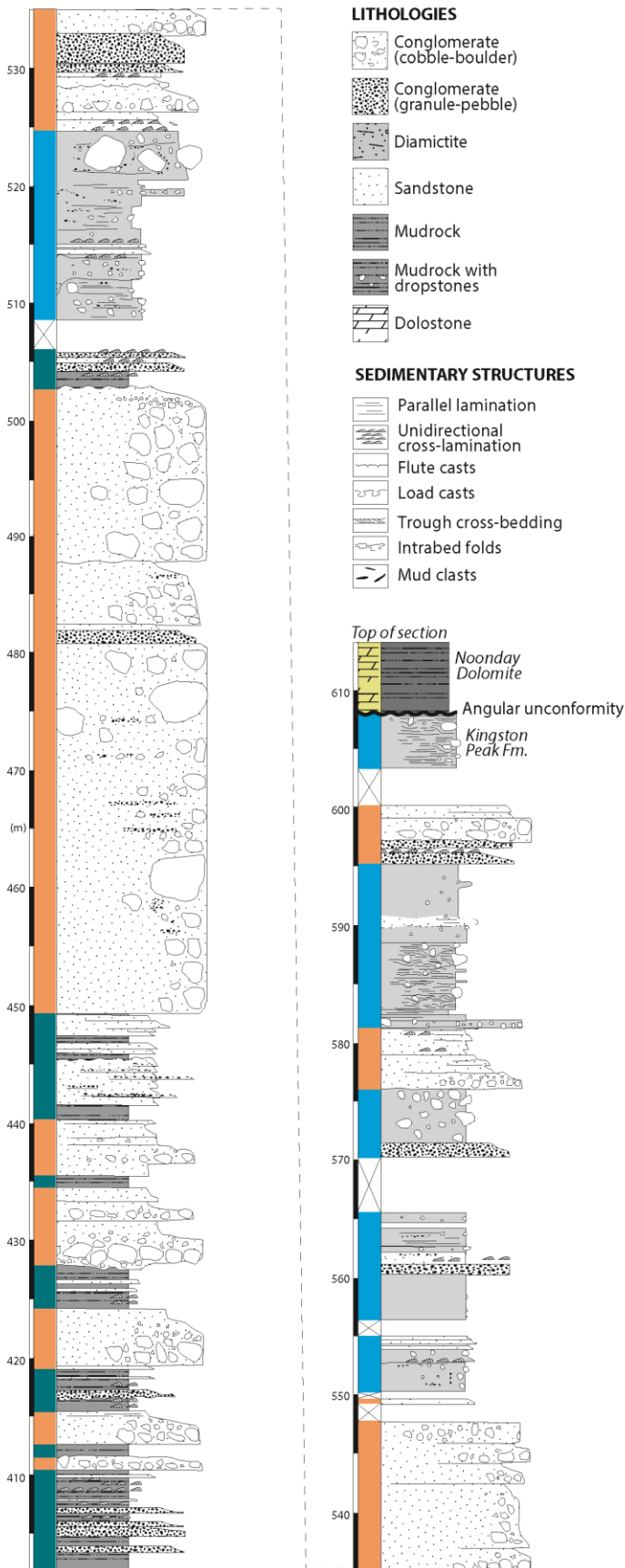


Figure 5 (part 2)

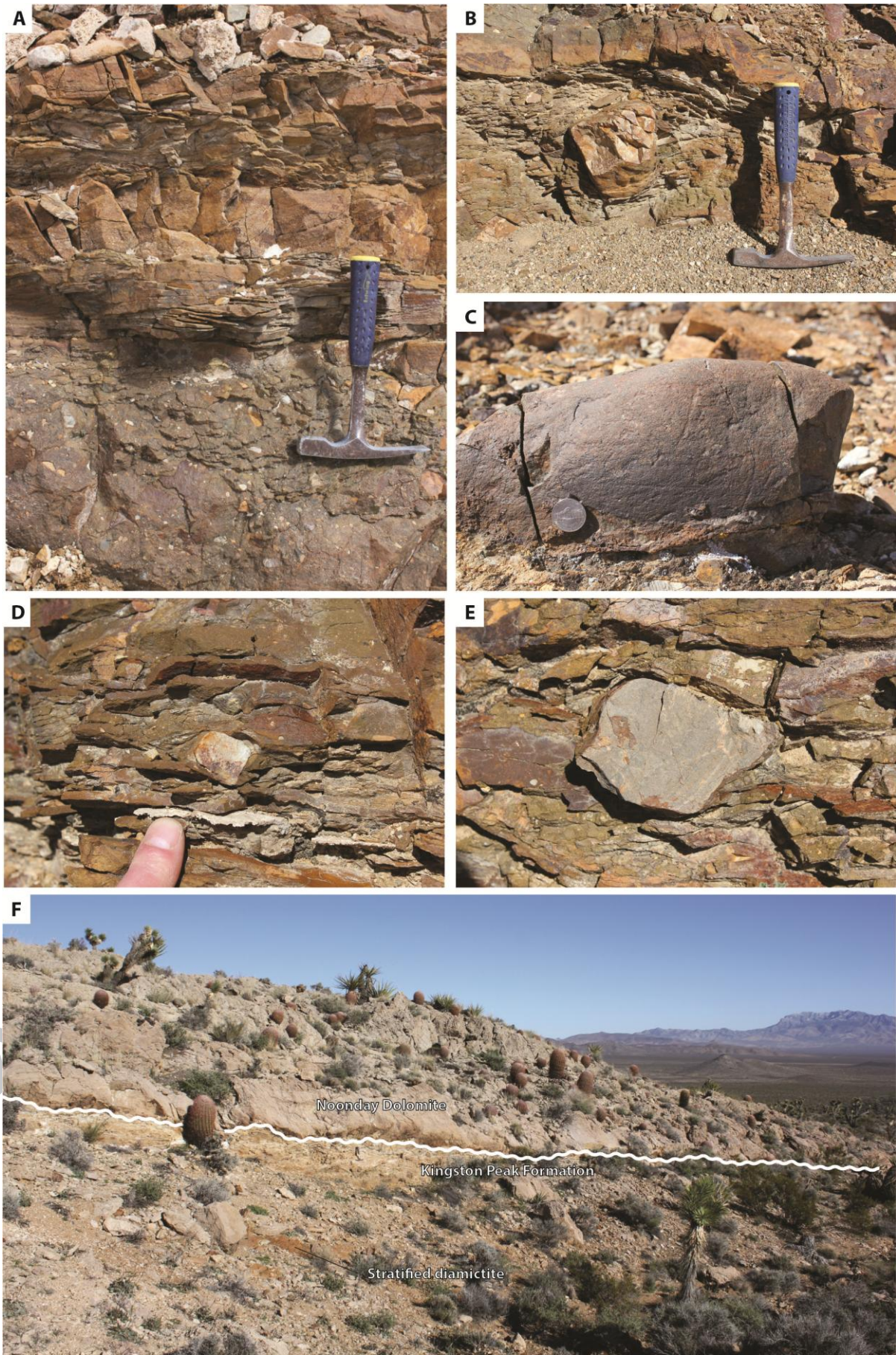


Figure 6

791

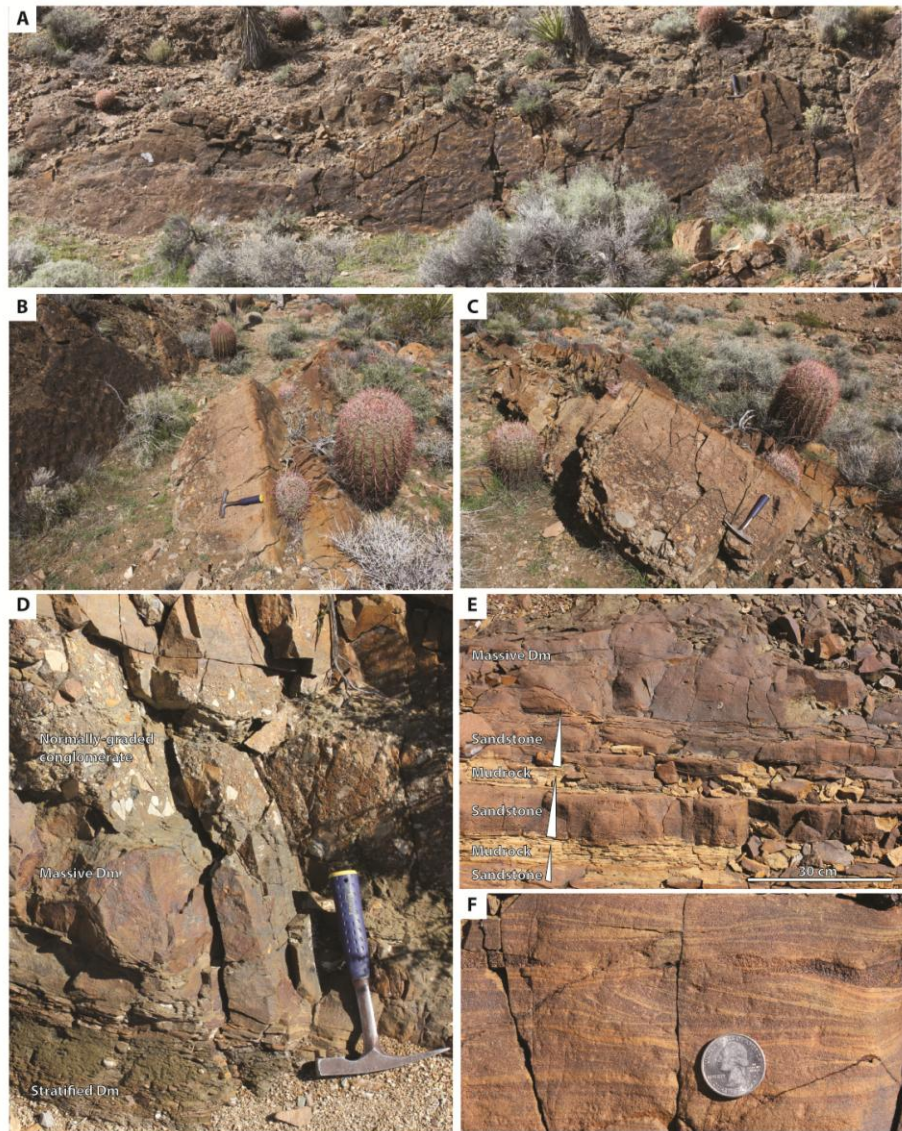


Figure 7

792

793

794

795

796

797

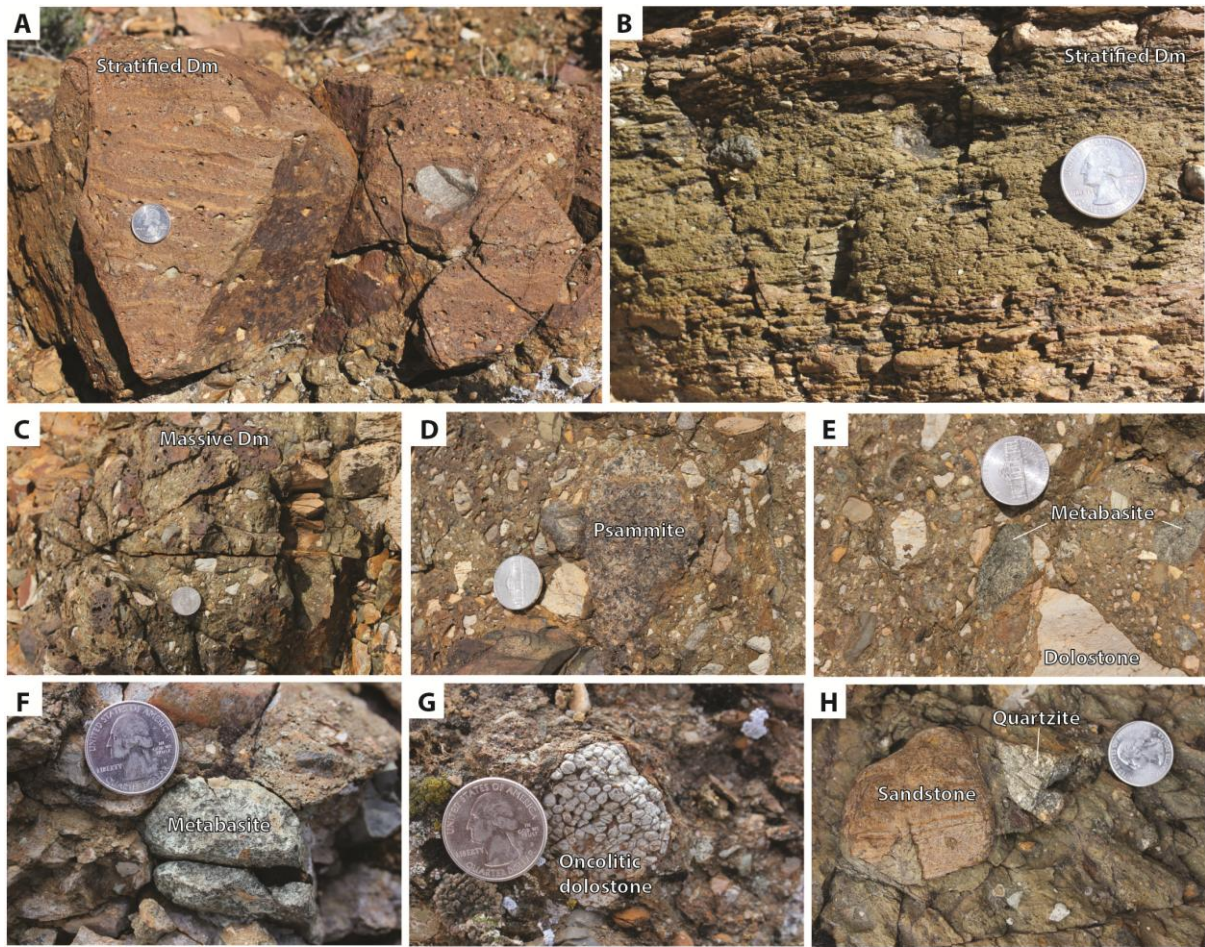


Figure 8

798

799

800

801

802

803

804

805

806

807

808

809

810

811

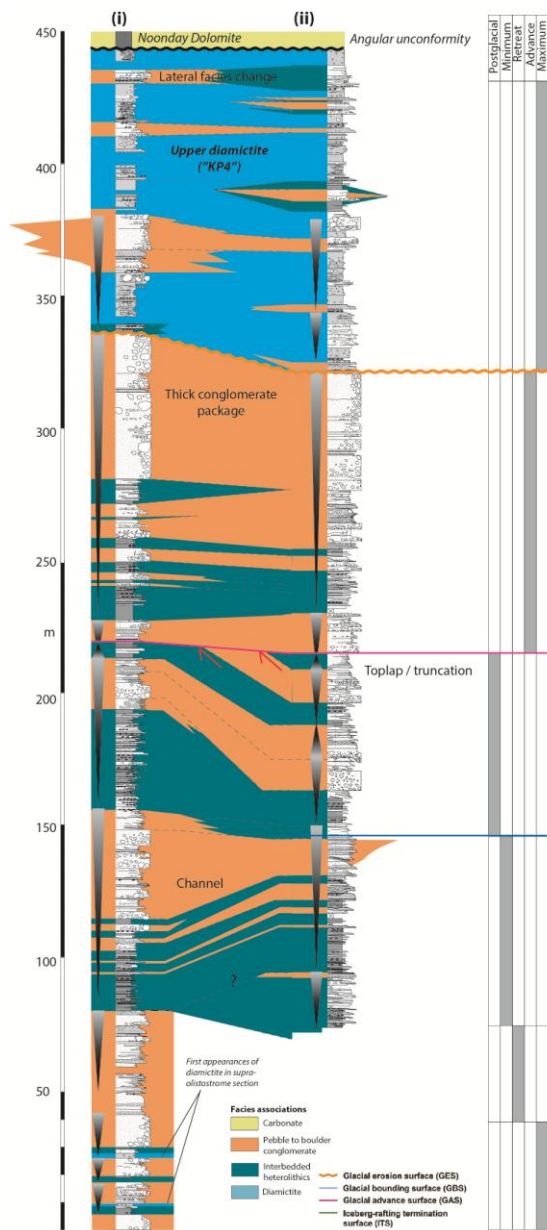


Figure 9

812

813

814

815

816

817

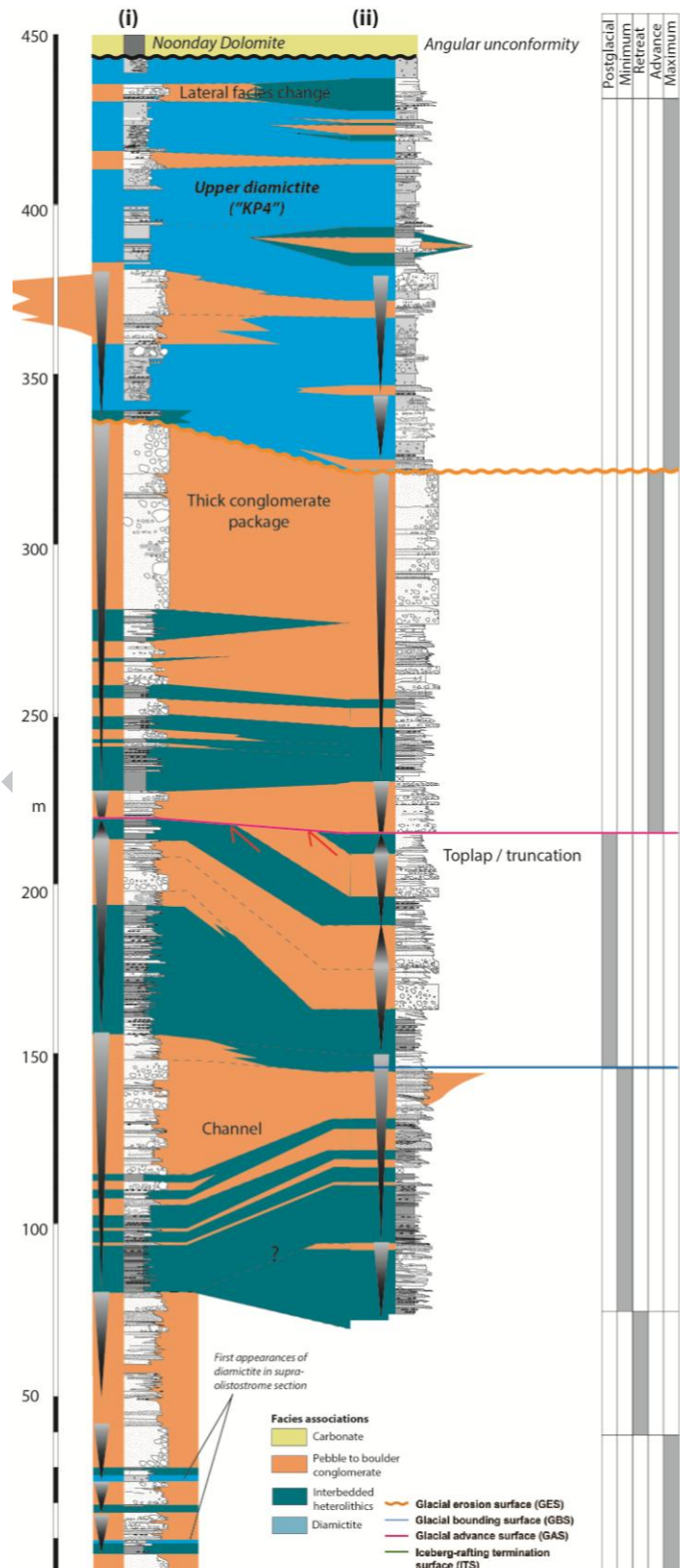
818

819

820

821 **Highlights**

- 822 • The sedimentology of the thickest
 823 succession of Cryogenian glacially-
 824 related strata in the Death Valley area-
 825 the Kingston Peak Formation (KPF)- is
 826 described in detail for the first time
 827 from the southern Kingston Range. The
 828 KPF is important as one of Laurentia's
 829 finest archives of Cryogenian
 830 glaciation, with the outcrop quality
 831 meriting consideration as a potential
 832 GSSP.
- 833 • In the southern Kingston Range, strata
 834 represent a major subaqueous fan
 835 complex that was deposited under the
 836 competing influence of rifting and
 837 glaciation.
- 838 • A sequence stratigraphic interpretation
 839 suggests that discrete phases of glacial
 840 advance, retreat, glacial maxima and
 841 glacial minima is proposed, which is
 842 useful to understand ice dynamics at a
 843 local scale.
- 844 • Uncertainty surrounds the
 845 stratigraphic value of many KPF
 846 subdivisions that have been previously
 847 proposed. This re-opens questions
 848 about representativeness and
 849 completeness of the Death Valley
 850 record.



851

852

853